Geo-Mar Lett
DOI 10.1007/s00367-017-0509-3

ORIGINAL

Morpho-sedimentary features and sediment dispersal systems of the southwest end of the Ryukyu Trench: a source-to-sink approach

Kan-Hsi Hsiung[1] · **Toshiya Kanamatsu**[1] · **Ken Ikehara**[2] · **Kazuya Shiraishi**[1] · **Chorn-Shern Horng**[3] · **Kazuko Usami**[2]

Received: 1 February 2017 / Accepted: 18 May 2017
© Springer-Verlag Berlin Heidelberg 2017

Abstract The southwestern Ryukyu Trench near Taiwan is an ideal place for source-to-sink studies because of the short sediment transport route between the terrestrial sediment source in Taiwan and the marine sink in the Ryukyu Trench. Bathymetric and seismic reflection data and core samples from the area around the southwestern Ryukyu Trench were used to identify features of the trench–arc system, including submarine canyons, the trench wedge, bathymetric ridges, and forearc basins, which together form two distinct sediment dispersal systems: a longitudinal (trench-parallel) system and a transverse (trench-normal) system. The longitudinal sediment dispersal system carries sediments eroded from the Taiwan orogenic belt eastward, primarily along the Hualien Canyon and a channel–terminal fan system at its mouth, and deposits them in the southwestern end of the Ryukyu Trench. The transverse sediment dispersal system carries sediments eroded from the Ryukyu Islands downslope and deposits them in the Hoping, Nanao, East Nanao, and Hateruma forearc basins, behind the barrier formed by the E–W-trending Yaeyama Ridge on the trench-slope break. The presence of pyrrhotite, a characteristic component of sediments sourced from Taiwan, in a seafloor sample from the Ryukyu Trench and its absence in a sample from the East Nanao forearc basin support the view that the southwestern Ryukyu Trench is longitudinally fed by sediment derived from Taiwan, whereas the trench-slope forearc basins receive sediment transported transversely downslope from the Ryukyu Islands.

✉ Kan-Hsi Hsiung
hsiung@jamstec.go.jp

[1] Japan Agency for Marine-Earth Science and Technology, 3173-25 Showa-machi, Kanazawa-ku, Yokohama, Kanagawa 236-0001, Japan

[2] Geological Survey of Japan, National Institute of Advanced Industrial Science and Technology, Central 7, 1-1-1 Higashi, Tsukuba, Ibaraki 305-8567, Japan

[3] Academia Sinica, Institute of Earth Sciences, Taiwan, Republic of China

Introduction

Oceanic trenches are the most significant elongate depressions on the seafloor of large subduction zones; they can be thousands of kilometers long, up to 8 km deep, and tens to hundreds of kilometers wide (Jarrard 1986; Stern 2002). In subduction zones, cross-sections of the tilted trenches illustrate the surficial and crustal processes of subduction and the deposition of deep-water turbiditic sediments in the trench (Karig and Sharman 1975). Trench-fill sediments are derived mainly from adjacent volcanic arcs and volcanic basins, and are transported to the trench by transverse submarine canyons (Karig and Sharman 1975; Underwood and Karig 1980). Some such trenches are filled by large volumes of terrigenous sediments. For example, the large trench wedge of the southern Chile Trench contains mainly orogenic sediments fed from the Andean continental margin by numerous submarine canyons transverse to the axis of the trench (Thornburg and Kulm 1987; Thornburg et al. 1990). Trenches are considered to be the ultimate sink for sediment dispersal systems along active margins such as the southern Chile Trench (Thornburg and Kulm 1987; Thornburg et al. 1990), the east Nankai Trough (Mountney and Westbrook 1996; Spinelli et al. 2007), and the northern Manila Trench (Yu et al. 2009; Hsiung and Yu 2011).

In general, the lateral terminations of trenches are formed by the combined effects of tectonic and sedimentary forcing at plate boundaries; most of them lie in areas that lack trench morphology and where subduction processes have probably

Published online: 29 May 2017

ceased. For instance, the western termination of the New Guinea Trench is at the N-trending seafloor rise known as the Mapia Ridge, and there is no clear indication there of modern subduction along the northern margin of New Guinea and insufficient data on the trench flanks to determine whether subduction has ever occurred there (Milsom et al. 1992). The morpho-sedimentary features at the ends of trenches reflect the combined effects of subduction, collision, and sedimentation processes. In particular, the amounts of accretion or erosion in modern convergent zones are determined mainly by the rate of plate convergence, sediment supply, and the topography of the subducting seafloor (Von Huene 1986). Where deposition in trenches is prevalent, the trench-fill deposits are controlled mainly by the rate of plate convergence, sediment supply, the presence of submarine canyons, and the gradient of the trench axis (Lash 1985). Pickering and Hiscott (2015) noted that trench-floor deposits are influenced by both lateral and longitudinal sediment supply. The various types of trench-fill deposits can be categorized according to their different settings and sediment transport paths (Macdonald 1993; Pickering and Hiscott 2015), but the ending of trenches has been overlooked. The wedge-shaped body of sediment (the trench wedge) that develops on the lower trench slope in front of the inner trench wall is a typical and distinct morpho-sedimentary feature of subduction zone trenches (Underwood and Karig 1980; Thornburg and Kulm 1987). The sediments in these wedges are sourced not only from the landward slope, but also by transport along the trench axis in response to gradual changes in bathymetry or bottom currents. The part of the wedge that is proximal to the accretionary prism is partly folded or thrust faulted and is later incorporated in the accretionary prism, which implies that tectonic activity (i.e., subduction) prevails over sedimentation. The lateral terminations of oceanic trenches can be investigated by using bathymetric data and seismic reflection profiles, which reveal the characteristic tectonic and sedimentary processes and the resultant morpho-sedimentary features. They have been used to define the northern limit of the Luzon Trough (the northern extension of the Philippine Trench) off the northeastern Philippine Islands (Hayes and Lewis 1984; Lewis and Hayes 1989). Similarly, bathymetric and seismic data have been used to identify the southern end of the South Shetland Trench near the Antarctic Peninsula, where it is associated with an inactive oceanic subduction zone (Maldonado et al. 1994; Gohl et al. 1997; Jabaloy et al. 2003).

Regional source-to-sink studies can facilitate an understanding of where and how terrestrial sediments are transported and deposited in a sink via sediment transport routes that entail various sedimentary processes. Oceanic trenches play an important role in source-to-sink studies (Sømme TO et al. 2009; Hinderer 2012). For example, the northern end of the Manila Trench in the northeastern South China Sea has been recognized as the ultimate sink of sediment derived from the Taiwan orogeny. A morpho-sedimentary feature developed there at water depths shallower than 4,000 m has progressively buried the typical trench morphology and laterally terminated the trench (Yu et al. 2009; Hsiung and Yu 2011; Hsiung et al. 2015). A large field of migrating sediment waves formed by turbidity currents covers an area of about 25,000 km^2 on the seaward slope of the northern end of the Manila Trench, and indicates that turbidite sedimentation prevails over subduction processes there (Damuth 1979). Other tectonic and sedimentary criteria have served to determine trench-end styles for, amongst others, the western Philippine Trench (Nichols et al. 1990; Milsom et al. 1992), and the eastern Sunda and New Guinea trenches (Milsom et al. 1992).

Taiwan's natural setting of high mountains, steep gradients, frequent earthquakes, erodible lithology, and heavy rainfall produces large amounts of sediment that are ultimately transported to the surrounding seas (Dadson et al. 2004, 2005; Milliman et al. 2007), including the adjacent southwestern Ryukyu Trench. The southwestern Ryukyu Trench is considered to be a sediment sink containing large amounts of sediment along the trench floor (Malatesta et al. 2013). Among known active margins, the Taiwan orogen and the nearby southwestern end of the Ryukyu Trench together provide an excellent area for source-to-sink studies. Much terrestrial sediment from Taiwan is transported over a relatively short distance and deposited in the adjacent Western Philippine Sea Basin and southwest Ryukyu Trench, thus facilitating investigation of the linkage between terrestrial source and marine sink (Fig. 1).

The aims of this study were to examine morpho-sedimentary features at the southwestern end of the Ryukyu subduction system and thereby elucidate sediment transport paths from eastern Taiwan to the southwestern Ryukyu Trench, and thus to contribute to a general model of trench sedimentation in similar tectonic settings. Bathymetric data, seismic reflection data, and sediment core analyses were used to achieve this aim. Two sediment dispersal systems were identified: a longitudinal (trench-parallel) system that carries sediments eroded from the Taiwan orogenic belt eastward into the western end of the Ryukyu Trench, primarily via submarine canyons; and a transverse (trench-normal) sediment dispersal system that carries sediments eroded from the Ryukyu Arc downslope and deposits them in a series of forearc basins behind the barrier provided by the Yaeyama Ridge on the shelf slope break.

Geological background

The Ryukyu Island Arc was formed as a consequence of subduction of the Philippine Sea Plate beneath the Eurasia Plate (Karig 1973; Angelier 1986). The Ryukyu subduction system extends 2,200 km southwest from Kyushu Island, Japan, to

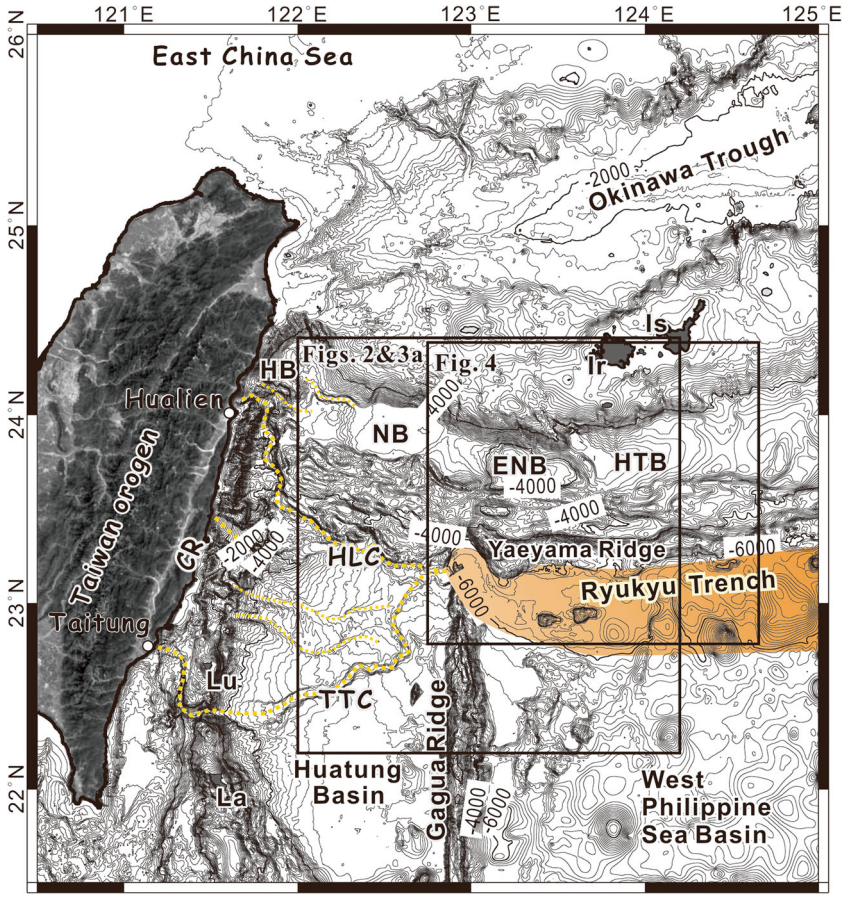

Fig. 1 Regional bathymetric map of the southwestern Ryukyu subduction zone between Taiwan and Iriomote Island. The southwest Ryukyu Trench (*orange*) terminates at the Gagua Ridge, which separates the Huatung and West Philippine Sea basins. Several large canyons (*yellow dotted lines*) incise the narrow slope off eastern Taiwan and extend into the Huatung Basin. A small canyon links the Hoping and Nanao basins. *CR* Coastal range, *HB* Hoping Basin, *NB* Nanao Basin, *ENB* East Nanao Basin, *HTB* Hateruma Basin, *Ir* Iriomote Island, *Is* Ishigaki Island, *HLC* Hualien Canyon, *TTC* Taitung Canyon, *Lu* and *La* Lutao–Lanyu Ridge (i.e., Luzon arc)

northern Taiwan, and includes the Ryukyu Trench, the Yaeyama accretionary prism, several forearc basins, the Ryukyu Islands, and several backarc basins (Dominguez et al. 1998; Schnürle et al. 1998a). The Philippine Sea Plate is converging with the Eurasia Plate at 61–78 mm/year from the eastern Ryukyu Trench to Taiwan (Smoczyk et al. 2013). The regional bathymetry at the western end of the Ryukyu Trench (Fig. 2) is indented by the northern part of the Gagua Ridge, which effectively closes the western end of the trench (Font et al. 2001). The Gagua Ridge is a relic of a failed subduction event during the Miocene in the western Philippine Sea Basin (Deschamps et al. 1998; Eakin et al. 2015). The N–S-trending Gagua Ridge extends along 123°E, is about 350 km long and 30 km wide, and separates the Huatung and West Philippine Sea basins (Fig. 1). Collision of the northern end of the Gagua Ridge with the forearc slope deformed the trench floor and adjacent accretionary wedge so that the trench floor and nearby accretionary prism were arched along a NW–SE axis (Fig. 1). Uplift of the forearc basins north of the convergent zone was also caused by the collision of the northern end of the Gagua Ridge with the forearc slope (Dominguez et al. 1998). Commonly cited examples of ridge–trench collisions in subduction zones include the collisions of the New Hebrides (Vanuatu) island arc with the North d'Entrecasteaux Ridge and the Bougainville Guyot (Collot and Fisher 1991; Underwood et al. 1995). The ridge–trench collision of the Bougainville Guyot deformed a broad area of the trench slope and uplifted the accretionary prism of the New Hebrides arc by about 2 km (Collot and Fisher 1991). Similarly, the landward slope of the southwestern Ryukyu Trench and the adjacent Yaeyama Ridge were deformed and uplifted by the northward collision of the Gagua Ridge. The southwestern Ryukyu Trench terminates in a curved fan-shaped trench floor east of the northern Gagua Ridge (Fig. 1). Subduction has ceased in the westernmost part of the Ryukyu subduction system, west of the Ryukyu Trench, although the oceanic crust of the northern Huatung Basin west of the Gagua Ridge is still actively subducting (Schnürle et al. 1998a).

The Taiwan orogenic belt (elevation 4,000 m), which lies at the junction of the Ryukyu subduction system and the Luzon arc, was formed by the oblique collision of the Luzon arc with the Chinese margin, which began during the late Miocene to early Pliocene (Suppe 1981; Ho 1986). The coastal range between Hualien and Taitung in eastern Taiwan reaches an elevation of about 1,500 m. Large volumes of orogenic sediments eroded from the Taiwan orogenic belt and the coastal range are transported eastward into the Huatung Basin along a network of submarine canyons that have deposited a thick sequence of sediments (~4 km) in the confined Huatung Basin (Yu 2003; Van Avendonk et al. 2014). The Taitung

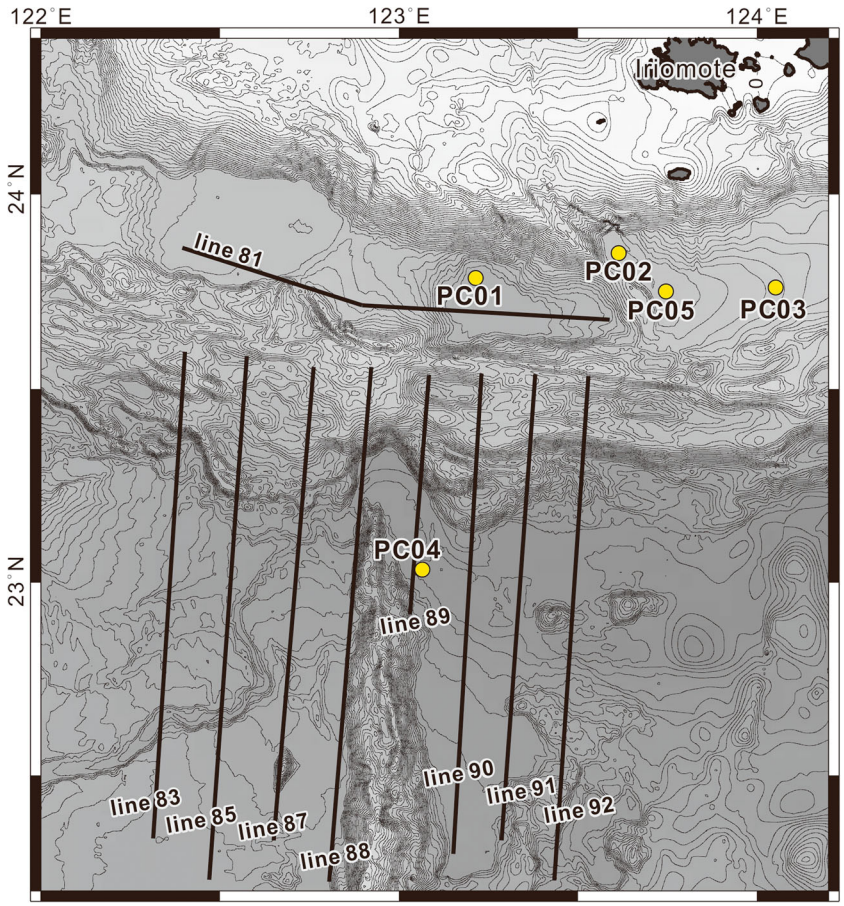

Fig. 2 Locations of nine seismic reflection profiles used in this study (cf. Fig. 1). The eight N–S profiles cross the western end of the Ryukyu Trench and northeastern marginal area of the Huatung Basin, and were used to identify morpho-sedimentary features and processes of regional sediment transport. The E–W profile crosses the Nanao and East Nanao forearc basins. *Yellow circles* Locations of five piston core samples collected in 2015 during R/V Kairei cruise KR15-18

and Hualien canyons are two major submarine canyons that originate at the mouths of rivers in eastern Taiwan (Dadson et al. 2005; Lehu et al. 2015). Numerous smaller east-trending submarine gullies provide a downslope drainage system on the eastern flank of the Luzon arc (Malavieille et al. 2002; Lehu et al. 2015). Other small canyons connected to minor rivers flowing eastward from the coastal range incise the lower western slope of the Huatung Basin (Lehu et al. 2015), and merge in their lower reaches as they approach the northern Gagua Ridge at the southwestern end of the Ryukyu Trench. The Gagua Ridge obstructs further sediment dispersal by submarine canyons off eastern Taiwan.

Forearc basins in the Ryukyu arc–trench system are important sites for deposition of sediments derived from the arc. Several forearc basins lie parallel to the southwestern Ryukyu Trench between the slope break and the toe of the slope (Fig. 1). Four of these are (from east to west) the Hoping, Nanao, East Nanao, and Hateruma basins (Aiba and Sekiya 1979; Okada 1989; McIntosh and Nakamura 1998; Lallemand et al. 1999). In the northeastern extension of this chain of forearc basins, east of Miyako Island, there has been rapid sedimentation (~360 cm/year) during the past ~150,000 years because of an enormous supply of sediment from the East China Sea and Ryukyu Arc (Ujiie et al. 1991). In addition, results from Holocene turbidite cores of the southern Ryukyu Trench slope suggested that the turbidity currents were possibly related to periodic earthquakes (Ujiie et al. 1997).

Materials and methods

The morpho-sedimentary features at the southwestern end of the Ryukyu Trench were determined in this study mainly from seismic reflection profiles and bathymetric data collected during the 1996 cruise of the Active Collision in Taiwan project and stored in the Ocean Data Bank (ODB) at the National Taiwan University, Taiwan. Eight down-dip seismic profiles across the western Ryukyu Trench and one profile parallel to the Ryukyu Trench axis across the Nanao and East Nanao basins were used for this study (Fig. 2). Nine bathymetric profiles across the Hualien Canyon and one along its thalweg (Fig. 3) were constructed from bathymetric data of ODB, Taiwan by using Generic mapping tools software (Wessel et al. 2013), and served to investigate the morphology of the seafloor at the western end of the trench. Swath bathymetric data collected south of Iriomote and Ishigaki islands in 2015 (Fig. 4) during cruises YK15-01 and KR15-18 of

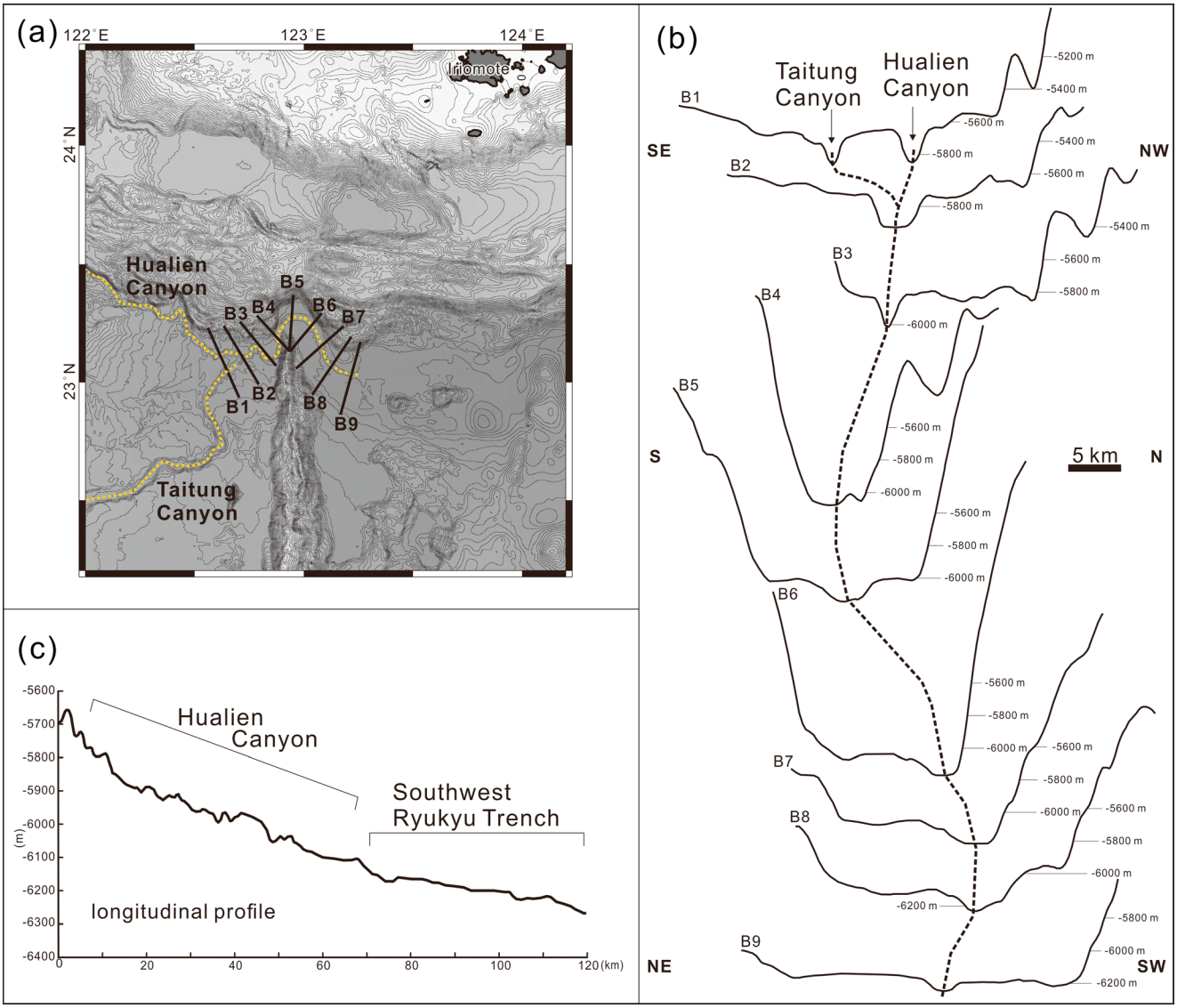

Fig. 3 **a** Locations of nine bathymetric cross-sections (*solid lines*) across the Hualien Canyon (*yellow dotted line*) and western end of the Ryukyu Trench (cf. Fig. 1). **b** Sequential bathymetric profiles across the Hualien Canyon showing progressive downstream changes of the route, width, and depth of the canyon. The merging of the Hualien and Taitung canyons west of the Gagua Ridge is also shown. **c** Longitudinal profile along the thalweg of the Hualien Canyon and into the western end of the Ryukyu Trench. Note the generally concave-up surface without a knickpoint

R/Vs Yokosuka and Kairei, respectively of the Japan Agency for Marine-Earth Science and Technology were used to improve mapping of the floor of the southwestern Ryukyu Trench (Fig. 4).

Five piston cores (PC01 to PC05) were collected in and north of the southwestern Ryukyu Trench during cruise KR15-18 (Fig. 2). Site PC01 is in the East Nanao Basin and site PC04 is in the western Ryukyu Trench (Fig. 2). Samples from the top of cores PC01 and PC04 were analyzed with a Quantum Design SQUID vibrating sample magnetometer (SQUID-VSM) at the Institute of Earth Sciences, Academia Sinica, Taiwan. SQUID analyses provide rapid identification of pyrrhotite in bulk samples on the basis of its low-temperature magnetic transition at 34 K. To avoid contamination, the uppermost undisturbed muddy intervals of each core were sampled. Samples from PC01 and PC04 were from depths of 12.5 and 9.2 cm below the seafloor, respectively. Samples were frozen, dried and weighted (ca. 0.2 g). To detect low-temperature magnetic transitions, the samples were cooled and their remanent magnetizations were measured from 300 K to 5 K in zero field in the SQUID-VSM. At 5 K, a 5 T DC field was applied and then switched off to impart a saturation isothermal remanent magnetization to the samples. The magnetization was measured again during warming in zero field.

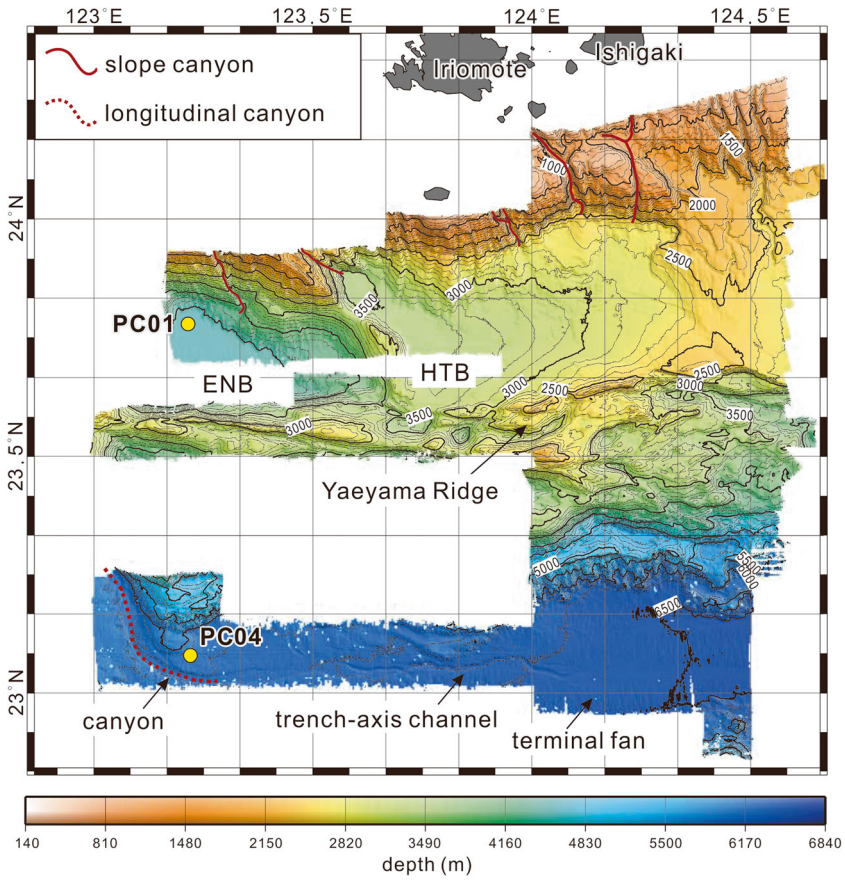

Fig. 4 Bathymetric map (100 m contours) derived from high-resolution data acquired south of the Iriomote and Ishigaki islands in 2015. *Red dotted line* Route of a canyon or channel about 100 km long on the floor of the Ryukyu Trench. *Solid red lines* Canyons descending the northern slopes of the East Nanao (*ENB*) and Hateruma (*HTB*) forearc basins. The Yaeyama Ridge, which is parallel to the trench axis, separates the forearc basins from the Ryukyu Trench

Results

Bathymetric features

The regional bathymetric map of the area offshore from eastern Taiwan (Fig. 1) shows a possible link between the southwestern end of the Ryukyu Trench and the Hualien Canyon, which extends landward and northwestward to a shallow coastal shelf near the city of Hualien. The longitudinal profile along the floor of Hualien Canyon and into the southwestern Ryukyu Trench (Fig. 3c) shows no definitive knickpoint at the transition from canyon to trench, indicating that the Hualien Canyon and southwestern end of the Ryukyu Trench are connected.

The series of approximately N–S-aligned bathymetric profiles (B1 to B9, Fig. 3b) show progressive changes in the morphology of the Hualien Canyon as it approaches and enters the western end of the Ryukyu Trench. The canyon forms a V-shaped valley about 3 km wide in profiles B1 to B3 (Fig. 3b). The V-shaped valley of the neighboring Taitung Canyon flows northward and merges with the Hualien Canyon between profiles B1 and B2. At profile B3, the V-shaped valley has widened and then becomes U-shaped and about 8 km wide on profile B4. Farther downslope, profiles B5 and B6 show the western Ryukyu Trench as a broad, roughly NW–SE-oriented U-shaped trough about 15 km wide and at ~6,000 m water depth, with a few shallow depressions along the axis of the trough. Farther eastward, the southwestern Ryukyu Trench widens (to ~20–30 km) to form an asymmetric trench with a steeper northern wall (profiles B7 to B9). There are shallow depressions along the trough axis, as indicated by the thalweg profile (Fig. 3b). The relatively flat trench floor of profiles B7 to B9 is at water depths of 6,100 to 6,250 m, with a lower west-to-east gradient than farther west and with only minor depressions along the trench thalweg (Fig. 3b). The longitudinal profile from the lower Hualien Canyon into the southwestern Ryukyu Trench (Fig. 3c) shows a slightly concave-up profile with minor irregularities.

The high-resolution swath bathymetric data collected south of Iriomote and Ishigaki islands in 2015 (Fig. 4) provide further strong evidence of a roughly trench-parallel canyon or channel extending from the Hualien Canyon in the northeastern Huatung Basin into the southwestern Ryukyu Trench, and support an argument for lateral supply (west to east) of sediment to the western Ryukyu Trench. The eastern termination of the slightly sinuous channel is at the edge of a flat fan-shaped area that can be interpreted to represent a terminal fan deposit. The distinct bathymetric characteristics of the interconnected canyon–channel–fan system (Fig. 4) are not evident in the older, lower-resolution bathymetric data (Figs. 1, 2, and 3). The thalweg of the longitudinal canyon

(red dashed line in Fig. 4) and linked deep-sea channel show clear braided patterns in the swath bathymetric data (Fig. 4).

The linear E–W-trending Yaeyama Ridge lies parallel to the trench at about 2,500 m water depth along the slope break between the trench floor and the East Nanao and Hateruma forearc basins. The maximum water depths of the East Nanao and Hateruma basins are about 4,600 and 3,500 m, respectively. Several submarine canyons extending from south of Ishigaki Island are likely avenues for sediment transport from the shallow continental shelf to the Nanao and East Nanao basins. However, none of these canyons or gullies crosses the trench-slope break (i.e., Yaeyama Ridge) in this region (Fig. 4).

Morpho-sedimentary features

This section summarizes interpretations of the eight N–S seismic reflection profiles across the Hualien Canyon and southwestern Ryukyu Trench, and the single trench-parallel profile across the Nanao and East Nanao basins. Lines 83 and 85 (Fig. 5) cross the Taitung and Hualien canyons and show truncated reflectors at the canyon walls, which rise ~800 m above the floor of the Taitung Canyon and ~550 m above that of the Hualien Canyon. Truncation of almost flat, parallel reflectors at the canyon walls (Fig. 5b and d) suggests that the strata there crop out in the canyon walls, indicating that the canyons were formed by erosional excavation of the shallow succession of the Huatung Basin. Stacked and contorted reflectors under both canyon floors are interpreted as multiple cut-and-fill features, implying multiple past erosion and deposition events in the canyons (Fig. 5b and d). The shallow successions along both profiles are layered and stratified seismic facies that extend to about 1.5 s two-way-traveltime (twt) below the seafloor in the northern part of the Huatung Basin and to 0.7 s twt below the seafloor in its southern part (Fig. 5a and c). The sediments thicken gradually northward and the channel of the Taitung Canyon swings northward. The chaotic seismic facies within the accretionary prism north of the Hualien Canyon suggest that the sediments accreted there represent the proto-Ryukyu Trench.

Farther down the canyon and just west of the Gagua Ridge, seismic lines 87 and 88 cross the mouth of the Hualien Canyon (Fig. 6), which takes the form of an irregularly shaped trough about 10 km wide. The canyon floor is characterized by hyperbolic diffraction patterns and chaotic seismic facies. On both profiles, the northern wall of the canyon is the seaward sloping surface of the Yaeyama accretionary prism, rather than the truncated strata of the Huatung Basin (Fig. 6a and c). Line 87 shows dominantly flat and parallel reflections in the shallow successions that extend to about 0.3 s twt below the seafloor of the Huatung Basin (Fig. 6a). The enlargement of the canyon mouth on line 87 shows multiple stacks of swells and bulges that represent multiple erosion/deposition events along the canyon floor (Fig. 6b). Line 88 shows that the mouth of the Hualien Canyon is about 10 km wide and lies between the northern end of the Gagua Ridge and the Yaeyama accretionary prism. The Gagua Ridge has a highly irregular topography as a result of its collision with the Yaeyama accretionary prism (Fig. 6c). The enlargement of the canyon mouth on line 88 (Fig. 6d) shows that the northern canyon wall is the seaward-sloping surface of the Yaeyama accretionary prism, whereas the southern canyon wall is the northernmost sloping flank of the Gagua Ridge. There are no truncated reflectors indicative of sediments cropping out on either of the canyon walls. The seismic characteristics of the canyon walls at the Hualien Canyon mouth imply that the canyon was formed mainly by tectonic forcing, rather than by erosional down-cutting of the sedimentary sequence (Fig. 6d). The confluence of the Hualien and Taitung canyons in the northeastern part of the Huatung Basin is a response to the slope, down to the north, of the basement of the Huatung Basin (Fig. 6a and c). Farther east on line 87 (Fig. 7a), the elongate depression of the Hualien Canyon gradually merges with a broader trough (~15 km wide) at the southwestern end of the Ryukyu Trench.

Line 89 traverses obliquely across the axis of the southwestern end of the Ryukyu Trench, and shows a tilted trench wedge confined between the Gagua Ridge and the Yaeyama accretionary prism (Fig. 7a). A small and shallow surface incision near the middle of the trench wedge indicates that there has been active erosional excavation of the trench floor there (Fig. 7a). On line 90 (Fig. 7b), the West Philippine Sea Basin is shown as a smooth, concordant and relatively flat succession that extends to about 0.5 s twt below the seafloor and thickens gradually northward. North of the West Philippine Sea Basin, there is a tilted trench wedge about 25 km wide with an irregular surface. The trench wedge succession south of the Yaeyama accretionary prism extends to about 1 s twt below the seafloor with a small and shallow erosional incision on its surface that is similar to, but wider than, the incision on line 89.

Lines 91 and 92 cross the floor of the Ryukyu Trench east of the Gagua Ridge, and show that the tilted trench wedge is confined between the Yaeyama accretionary prism to the north and the West Philippine Sea Basin to the south (Fig. 8). The trench wedge sediments extend to about 1.1–1.2 s twt (red lines on Fig. 8) below the seafloor. The relatively flat surface of the trench wedge is cut by a small erosional channel, indicating minor erosion and active sediment transport (Fig. 8a). The shallow and thin succession of the West Philippine Sea Basin extends to about 0.5 s twt below the seafloor and is erratically punctuated by volcanic intrusions (Fig. 8a). The trench wedge as shown on line 92 (Fig. 8b) is similar but thicker than on line 91; the sedimentary succession there extends to about 2 s twt below the seafloor. It has a relatively flat surface and is again cut by an erosional incision (Fig. 8b). The northern part of the trench wedge has been folded and partly

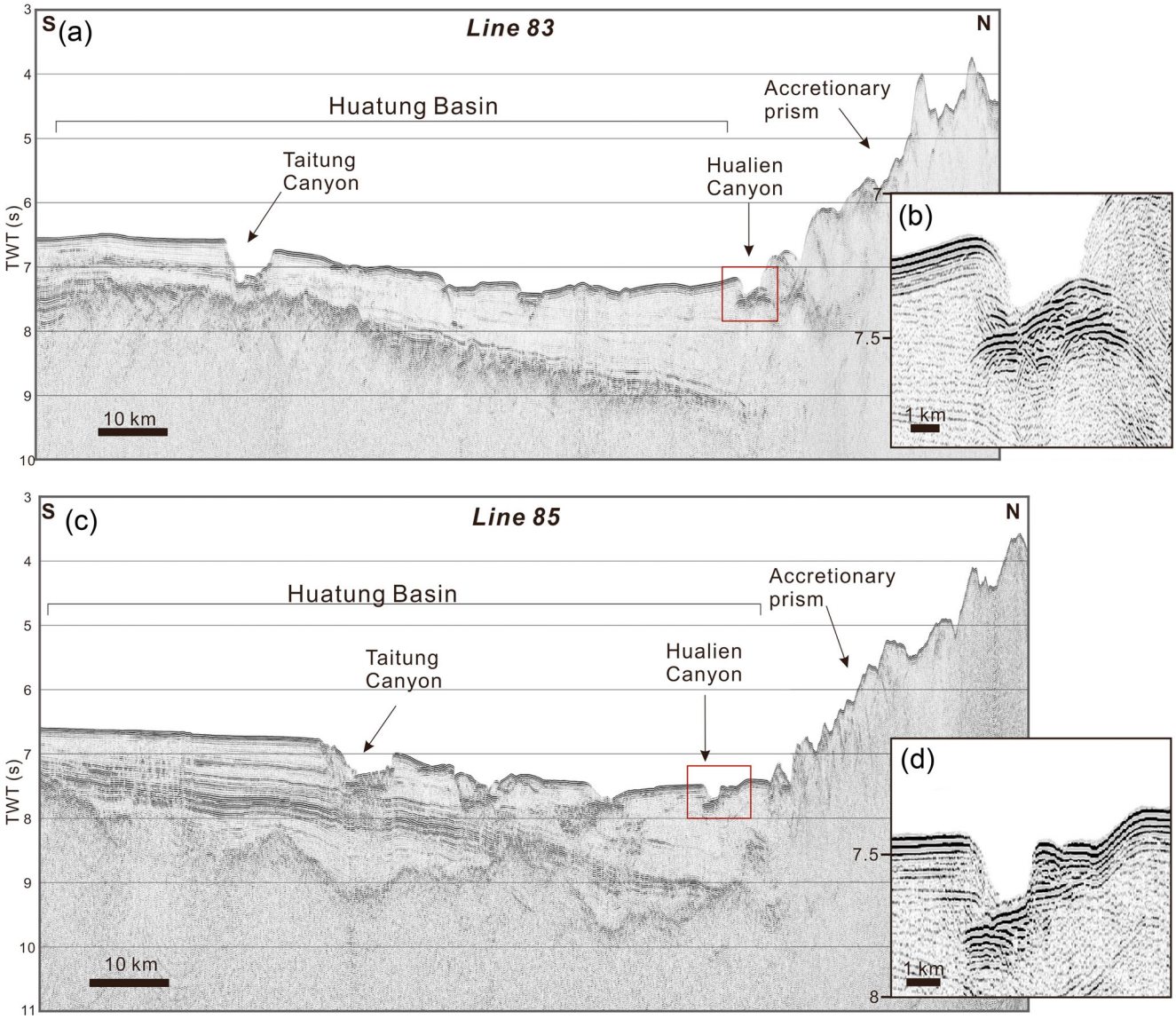

Fig. 5 Seismic reflection profiles along lines 83 and 85 in the Huatung Basin parallel to the Gagua Ridge and crossing the Hualien and Taitung canyons. **a** Line 83 and **b** an enlargement showing that the Hualien Canyon is about 3 km wide with walls about 550 m high. **c** Line 85 and **d** an enlargement showing that the Taitung Canyon is about 5 km wide with walls about 800 m high. For locations of seismic profiles, see Fig. 2

incorporated in the lower trench slope of the Yaeyama accretionary prism, indicating the effect of tectonic compression (Fig. 8b). East of the Gagua Ridge, the sedimentary wedge is clearly and continuously developed along the trench axis at the base of the trench slope (Figs. 7 and 8).

The eight trench-normal seismic profiles across the southwestern end of the Ryukyu Trench clearly identify two distinct morpho-sedimentary features with different dominant processes: (1) in its lower reaches, the dominant processes along the Hualien Canyon west of the Gagua Ridge are erosion and transportation; (2) east of the Gagua Ridge, the dominant process is deposition to form the sedimentary wedge. The shallow sedimentary succession of the Huatung Basin extends to about 1.5 s twt below the seafloor and is considerably thicker than the succession of the West Philippine Sea Basin, which extends to only about 0.5 s twt below the seafloor.

Seismic line 81, north of the Ryukyu Trench and parallel to the strike of the southwest Ryukyu subduction system (Figs. 2 and 9), reveals the seismic characteristics and sedimentary features of the Nanao and East Nanao forearc basins (Fig. 9). The floors of the Nanao and East Nanao basins are at water depths of 3,700 and 4,600 m, respectively. The basin sequences are characterized by smooth and roughly parallel flat reflections that onlap the basement at the basin margins. The stratified sedimentary successions of the Nanao and East Nanao basins extend to about 1.2 and 0.8 s twt, respectively below the seafloor (Fig. 9).

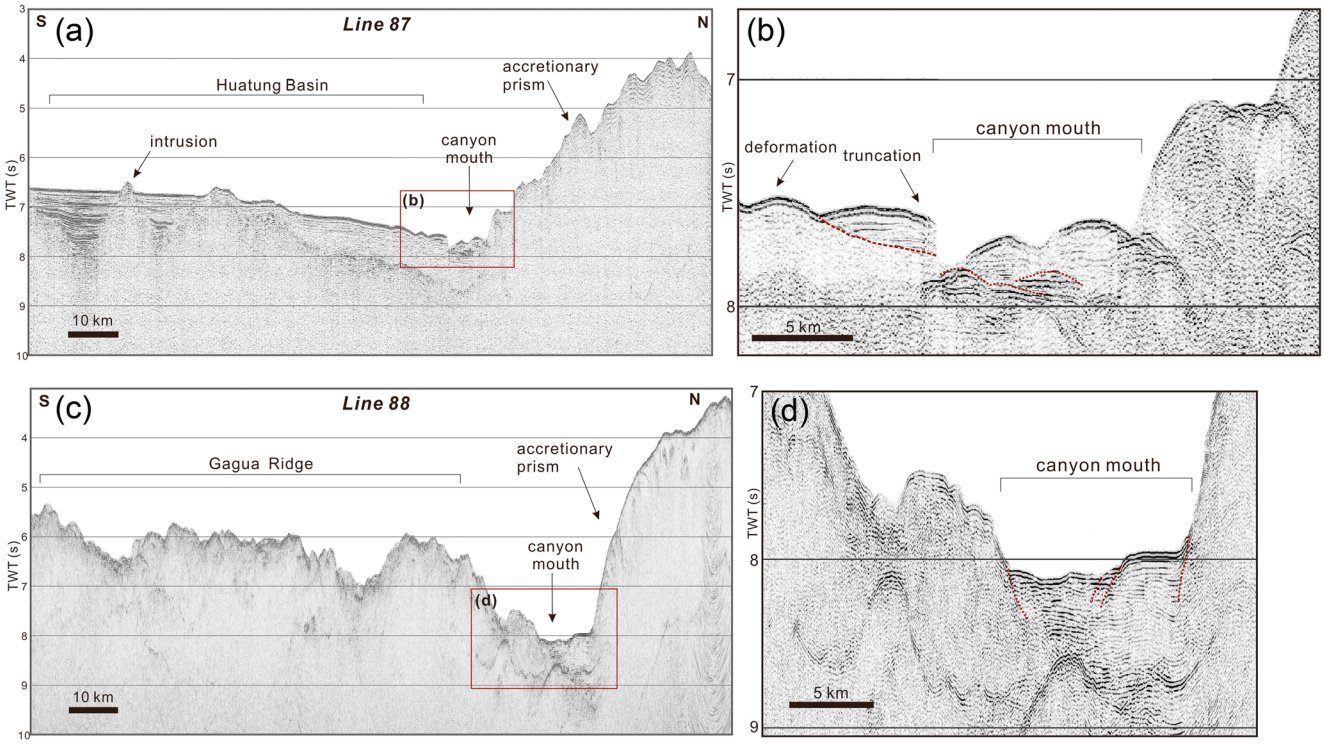

Fig. 6 Seismic reflection profiles along lines 87 and 88 (locations in Fig. 2), which cross the lower Hualien Canyon and canyon mouth west of and parallel to the Gagua Ridge. **a** Line 87 and **b** an enlargement showing the canyon mouth to be about 10 km wide with cut-and-fill features on the canyon floor. Swells (*red dotted lines*) on and under the canyon floor suggest multiple erosion and deposition events. **c** Line 88 and **d** an enlargement showing that the canyon mouth is about 10 km wide, and that the Gagua Ridge and Yaeyama accretionary prism form the southern and northern canyon walls, respectively, suggesting that the canyon formed in response to tectonic forcing. In **d**, chaotic seismic facies are observed within both canyon walls

SQUID-VSM measurements

Detrital pyrrhotite can be used as a tracer in investigations of the processes of sediment transport from terrestrial landmasses to submarine basins (Horng and Roberts 2006; Horng et al. 2012). Detrital pyrrhotite episodically eroded from the Taiwan orogenic belt during the Plio-Pleistocene may be preserved in adjacent marine sedimentary basins (Horng et al. 2012). Piston core samples from the East Nanao Basin and Ryukyu Trench floor were analyzed to test the hypothesis that sediments eroded from the Taiwan orogenic belt have been transported to and deposited in the southwestern Ryukyu Trench.

The results of magnetic susceptibility analyses of core samples from the East Nanao Basin (core PC01, 4,577 m water depth, Fig. 2) and the western Ryukyu Trench (core PC04, 6,147 m water depth) are shown in Fig. 10. The core recovery is 5.04 mbsf for PC01 and 3.23 mbsf for PC04. Both analyses show clear peaks indicative of the low-temperature transition of magnetite at 119 K (Abrahams and Calhoun 1953). For core PC01, the peak is not at exactly 119 K (Fig. 10b), which can be attributed to the low density of magnetic clay minerals. A low-temperature magnetic transition at 34 K provides positive evidence of the presence of monoclinic pyrrhotite (Rochette 1987; Dekkers et al. 1989); this transition is clearly shown in the analyses of the sample from core PC04 from the Ryukyu Trench (Fig. 10c and d), but is absent for the sample from core PC01 from the East Nanao Basin (Fig. 10a and b).

Discussion

Longitudinal sediment dispersal

The bathymetric mapping and interpreted seismic profiles presented here show strong evidence of a previously unknown regional along-strike seafloor sediment transport route between the deepest part of the seafloor along the Ryukyu subduction zone and the Taiwan collision zone (Fig. 3). The southwestern end of the Ryukyu Trench appears to receive sediment from the mouth of the Hualian Canyon, which extends northwestward and landward to the northern end of the coastal range in eastern Taiwan (Fig. 1). In the context of source-to-sink analysis (MARGINS 2004; Sømme TO et al. 2009; Covault et al. 2011), the Ryukyu Trench wedge is the ultimate sink of sediments fed longitudinally along the Hualien Canyon, which is the major sediment conduit within a longitudinal sediment dispersal system along the Taiwan–Ryukyu subduction system.

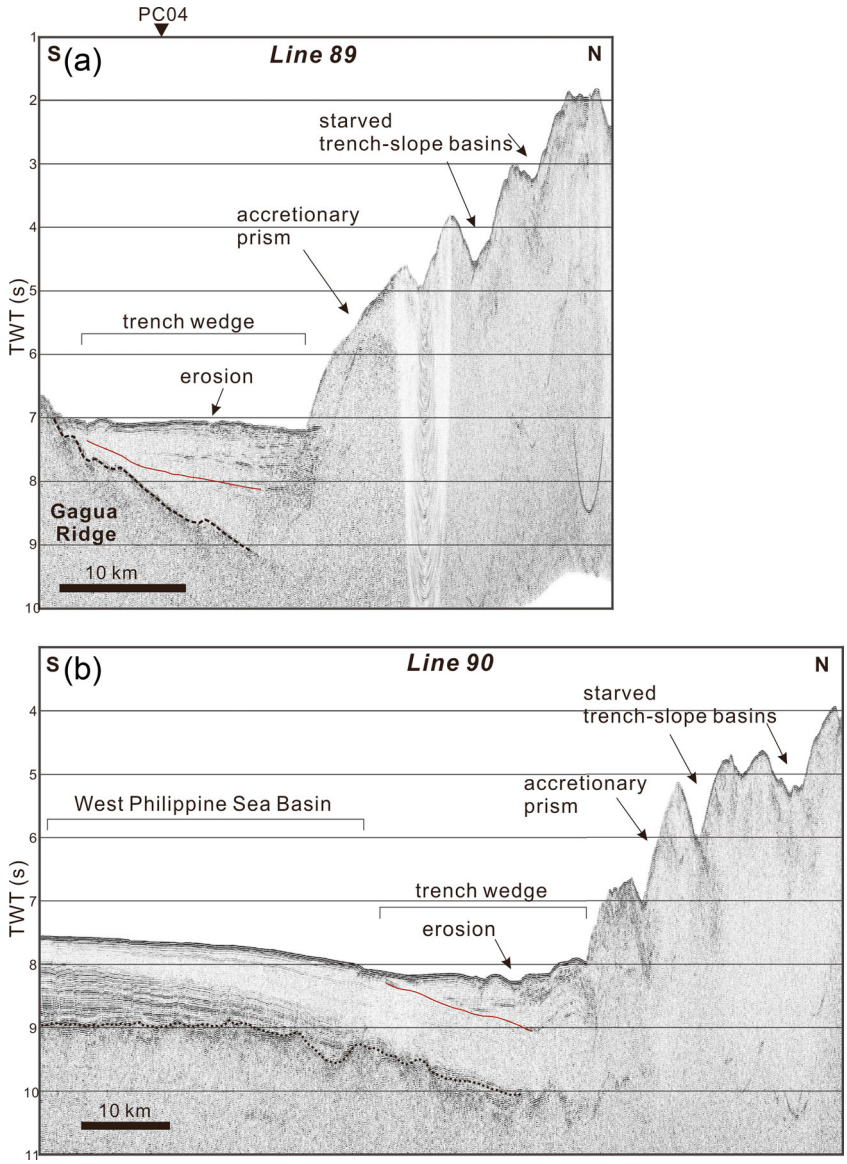

Fig. 7 Seismic reflection profiles along lines 89 and 90 across the southwest end of the Ryukyu Trench. **a** Line 89 obliquely crosses the end of the Ryukyu Trench, showing the trench wedge to be about 20 km wide and 1 s twt thick. A relatively small axial incision appears on the trench wedge floor, indicating minor erosion and active sediment transport. **b** The trench wedge appearing on line 90 is about 25 km wide and about 1 s twt thick with an irregular surface. The trench wedge bottom (*red line*) gradually merges southward to the floor of the West Philippine Sea Basin. Several starved trench-slope basins occur on the Yaeyama accretionary prism north of the trench wedge. *Dotted black line* Basement

The merging of the Taitung Canyon with the lower Hualien Canyon is an important component of lateral supply of sediment to the longitudinal dispersal system. River-connected canyons off the east coast of Taiwan, such as the Hualien River–Hualien Canyon, Hsiukuluan River–Chimei Canyon, and Peinan River–Taitung Canyon (Dadson et al. 2005), are very effective sediment conduits that supply large volumes of terrestrial sediment by simple downslope processes or along submarine canyons that traverse the slope offshore from the coastal range to the Huatung Basin (Malavieille et al. 2002; Lehu et al. 2015). These large canyons form a drainage network within the Huatung Basin, where they erode surface sediments on the seafloor, move them downslope, and provide effective pathways for transport and deposition of sediments from Taiwan.

The Hualien Canyon provides the major longitudinal route for delivery of terrestrial sediments from the Taiwan orogenic belt to the southwestern end of the Ryukyu Trench (Fig. 11). Longitudinal transport is an important component of sediment dispersal from mountain sources to oceanic sinks (i.e., trenches) in subduction systems along convergent margins (Su et al. 2015). For example, in the Solomon Sea, the Markham canyon–channel system merges with the southwestern New Britain Trench, and feeds sediments derived from the Finisterre Range longitudinally to the trench (Whitmore et al. 1999; Hsiung and Yu 2013). In both the Taiwan Orogen–South China Sea and Finisterre Range–Solomon Sea regions, sediments from a terrigenous source are transported mainly longitudinally to an oceanic trench via a canyon–channel system. In its upper reaches, the Hualien Canyon is oriented generally N–S before turning sharply to the southeast at a water depth of ~2,000 m; the canyon then continues southeastward until it merges with the western end of the Ryukyu Trench at a water depth of ~6,000 m. Near Taiwan, the northern wall of the Hualien Canyon is confined by the curved frontal slope of the

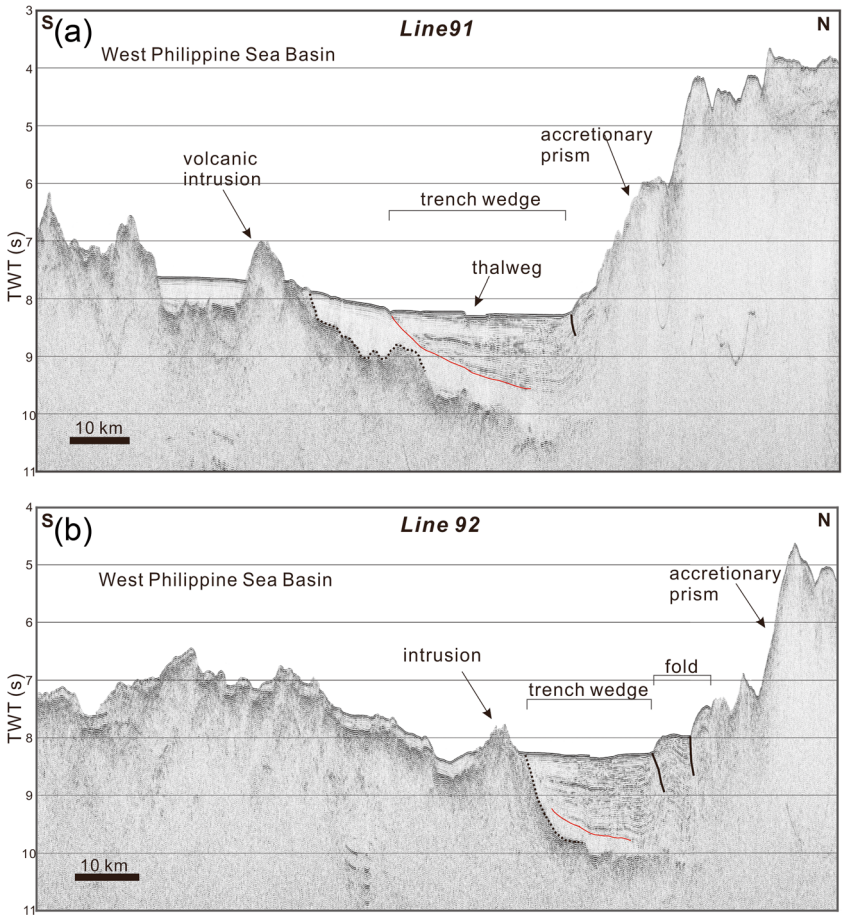

Fig. 8 Seismic reflection profiles along lines 91 and 92 (locations in Fig. 2) across the Ryukyu Trench east of the Gagua Ridge. **a** Line 91 shows a typical trench wedge south of the Yaeyama accretionary prism that thins toward the outer trench slope. The trench wedge has a relatively flat surface with a clearly defined thalweg, is about 30 km wide, and the sedimentary succession extends to about 1.1 s twt below the seafloor. **b** Line 92 shows the trench wedge to be about 20 km wide with the sedimentary succession extending to about 1.2 s twt below the seafloor. The sediments close to the accretionary prism are folded and thrust faulted, and have been incorporated in the Yaeyama accretionary prism. The surface of the West Philippine Sea Basin is punctuated by intrusions manifested as irregular peaks on the seafloor. *Red line* Base of trench wedge, *black dotted line* basement, *black solid line* thrust faults

Yaeyama accretionary prism (Fig. 1). Recurring failures of deep-water cables crossing the Huatung Basin suggest there may be periodic flows of turbidity currents in the submarine canyons on the slope offshore from eastern Taiwan; these might accelerate transport of sediments from eastern Taiwan to the Huatung Basin (Soh et al. 2004). Similarly, turbidity currents in the lower reaches of the Hualien Canyon might deliver sediments to the western Ryukyu Trench.

The course of the Taitung Canyon is strongly influenced by the topography of the seafloor of the Huatung Basin. From its head, the Taitung Canyon extends eastward toward the sea for about 170 km, and then swings sharply south to follow the southward-tilted western flank of the N–S-trending Lutao–Lanyu Ridge. It then swings to the east, crosses the Lutao–Lanyu Ridge, and then maintains a roughly northeastward course into the

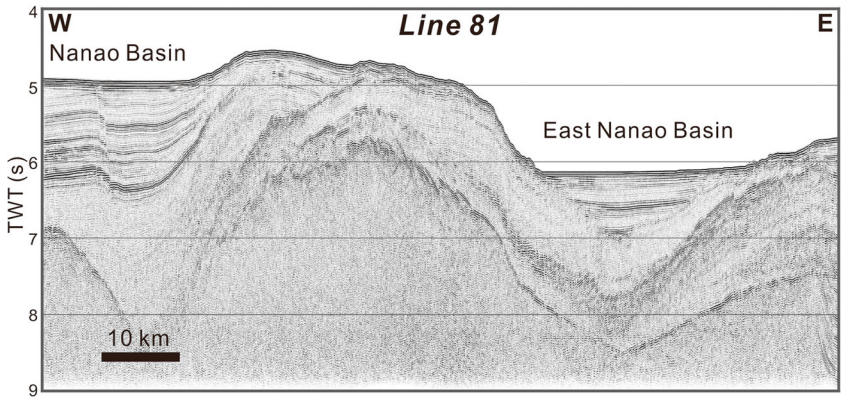

Fig. 9 Trench-parallel seismic reflection profile along line 81 across the Nanao and East Nanao basins (location in Fig. 2). The stratified basin-fill sediments extend to about 1.2 and 0.8 s twt below the seafloor in the Nanao and East Nanao basins, respectively. The basin-fill successions are characterized by smooth, mainly flat and roughly parallel reflections that onlap on the basement at the basin margins

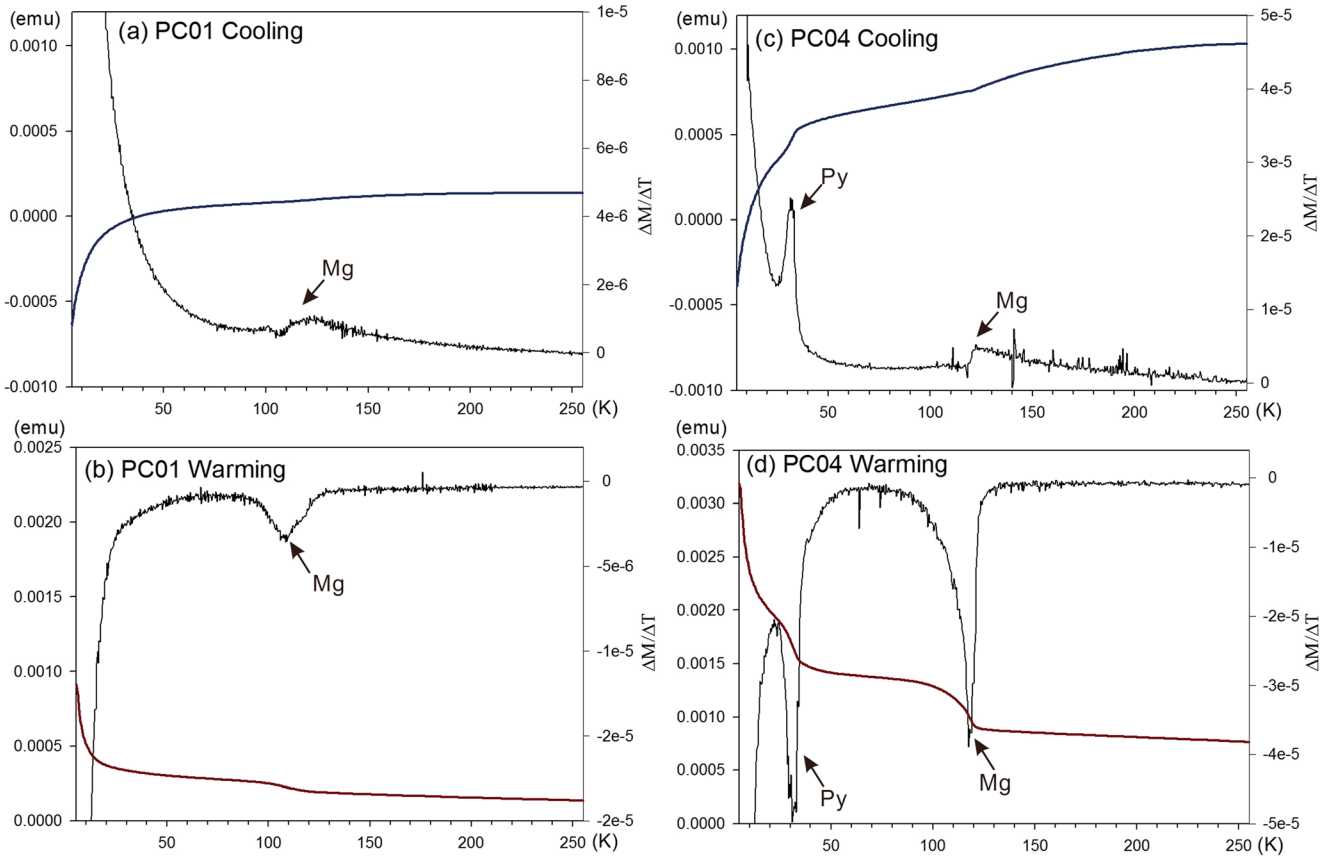

Fig. 10 Results of magnetic susceptibility analyses of bulk marine sediments from cores PC01 (East Nanao Basin) and PC04 (southwestern Ryukyu Trench floor) measured by SQUID VSM over temperatures from 5 K to room temperature. Both heating and cooling rates were 3 K/min. The magnetic susceptibility scale (emu) on the left-hand of each plot has been converted to ΔM/ΔT on the right-hand side. The magnetic transitions at 119 K indicate that there is magnetite (Mg) in the sediments from both cores. The magnetic transition at 34 K for only the sample from PC04 indicates that there is pyrrhotite (Py) in the sediments of the southwestern Ryukyu Trench, but not in those from the East Nanao Basin

Huatung Basin deep before turning sharply north and merging with the lower reaches of the Hualien Canyon (Schnürle et al. 1998b). The abrupt change in direction from northeast to north appears to be a response to a change of the downward slope of the basin floor from northeast to north. The network of submarine canyons off the eastern coast of Taiwan allows terrestrial sediments from the Peinan River drainage basin in the southernmost coastal range near the city of Taitung to be transported deep into the Huatung Basin.

The N–S-trending Gagua Ridge is a significant barrier within the sediment dispersal system of the southwestern Ryukyu Trench; it blocks the transport of terrestrial sediments derived from the Taiwan orogenic belt into the West Philippine Sea Basin. Consequently, most of those sediments are deposited within the Huatung Basin. East of the Gagua Ridge, the floor of the West Philippine Sea Basin is almost devoid of sediments derived from the Taiwan orogenic belt. The only route for transport of sediments eastward out of the Huatung Basin is via the Hualien Canyon and the channel that connects it to the southwestern Ryukyu Trench.

Trench wedge sedimentation

Oceanic trenches can be filled with sediments by a variety of sedimentary processes (Underwood and Karig 1980; Thornburg and Kulm 1987; Thornburg et al. 1990; Underwood et al. 1995; Pickering and Hiscott 2015). Gullies, closely spaced across the trench slope, deposit sediments directly onto the trench floor at the base of the trench slope. The mouths of large submarine canyons can act as point sources that deliver terrigenous sediments directly to the trench floor, bypassing depositional sites such as trench-slope basins along the lower slope. Much of the sediment on the trench slope is transported by downslope processes and mass-wasting perpendicularly to the trench floor. Trench-floor sediments can be transported along the trench axis by channels that follow the regional longitudinal gradient. In addition to longitudinal sediment transport in channels along the axis of the trench (e.g., Chile Trench; Thornburg and Kulm 1987), large volumes of sediment can be laterally fed to the ends of trenches by channels or canyons. For example, the

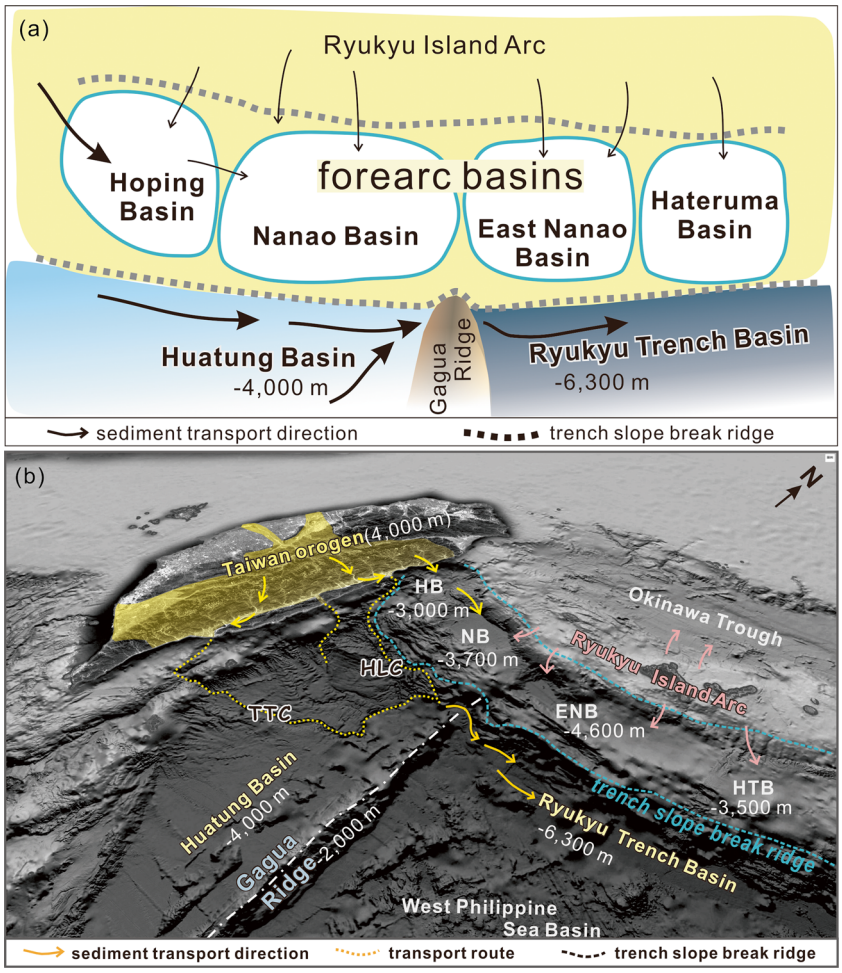

Fig. 11 **a** Source-to-sink diagram showing the two sediment dispersal systems in the southwestern Ryukyu subduction system: longitudinal transport of sediments along the trench, and transverse transport of sediments into forearc basins. **b** 3-D image of seafloor topography showing the interconnected Hoping (*HB*), Nanao (*NB*), East Nanao (*ENB*), and Hateruma (*HTB*) forearc basins, which are aligned parallel to the plate boundary. The Yaeyama Ridge follows the trench-slope break at the 2,500 m bathymetric contour (*blue dashed line*) and separates the forearc basins from the Ryukyu Trench. The ridge provides a barrier to downslope transport of sediments derived from the Ryukyu Arc (*pink arrows*) into the trench and Huatung Basin. Most of the sediments derived from the Taiwan orogenic belt (*yellow arrows*) are transported longitudinally to the Ryukyu Trench. *Yellow shading* Distribution of pyrrhotite in surface sediments of Taiwan, *HLC* Hualien Canyon, *TTC* Taitung Canyon

northern end of the Manila Trench is connected to the Penghu canyon–channel system, which provides a longitudinal source of sediments derived from the Taiwan orogenic belt to the northern Manila Trench in the South China Sea (Hsiung and Yu 2011); this shows the importance of the longitudinal supply of sediments that form trench wedges. It appears that seafloor topography, sediment supply, the presence or absence of submarine canyons and channels, the locations and orientations of submarine canyons, and the gradient along the trench axis are the major factors that control deposition in trenches and the formation of trench wedges in subduction zones. For example, the Hikurangi Channel along the axis of the Hikurangi Trench east of New Zealand forms a 1,500-km-long sediment conduit that feeds sediment into the southwest Pacific Basin (Lewis 1994). In the northern Philippine Sea Basin, the Zenisu deep-sea channel along the trough axis provides a pathway for terrigenous and shallow-marine sediments from central Japan to be transported to the Zenisu Trough (Wu et al. 2005). Both of these examples show the significance of longitudinal sediment transport for the deposition of trench wedges.

At the western end of the Ryukyu Trench, east of the Gagua Ridge, a continuous and distinctly wedge-shaped sediment body has developed on the trench floor (Figs. 7 and 8). The trench wedge is 20–30 km wide and contains a sedimentary sequence that extends to 0.5–1.2 s twt below the seafloor, and is bounded to the north by the Yaeyama accretionary prism and to the south by the Western Philippine Sea Basin. The trench wedge within the southwestern Ryukyu Trench appears to contain sediments from two sources: the major component is terrestrial sediments from Taiwan that have been transported from the Huatung Basin, with a minor component of pelagic sediments from the West Philippine Sea Basin.

A schematic representation of the relationships among the factors that control sedimentation in the southwestern Ryukyu Trench is provided in Fig. 11. There are no submarine canyons or channels to provide sediment pathways across the Yaeyama accretionary prism and forearc basins to the trench (Fig. 1), so only little sediment from the proximal sources of the Ryukyu islands and Yaeyama accretionary prism could be transported to the trench by these means. However, several small, starved trench-slope basins on the lower slope of the Yaeyama accretionary prism (Figs. 7 and 8) indicate that small amounts of

sediment are transported downslope (e.g., by mass-wasting), some of which may reach the trench floor to form hemipelagic deposits. The trench-parallel, linear Yaeyama Ridge provides a barrier to downslope transport of sediments sourced from the Ryukyu Islands, which are instead trapped behind the ridge, where they form forearc basins (Fig. 11), and further restrict the supply of sediment to the starved trench-slope basins farther downslope. The low-lying seafloor of the Western Philippine Sea Basin south of the Ryukyu Trench is draped by a thin sheet pelagic facies (Fig. 8a and b), which is relatively stable and, in the absence of submarine canyons, not easily eroded and transported to the Ryukyu Trench floor.

The source and transport route for sediments in the trench wedge in the southwestern Ryukyu Trench are quite different from those of trench wedges in the Middle America Trench (Underwood and Karig 1980) and southern Chile Trench (Thornburg and Kulm 1987; Thornburg et al. 1990), where the trench wedges receive sediments from large individual submarine canyons, or closely spaced smaller channels, which cross the trench slope and deliver sediments directly (laterally) to the trench floor. In contrast, much of the sediment derived from the Taiwan orogenic belt is transported longitudinally to the western end of Ryukyu Trench by the Hualien Canyon, which itself receives sediment laterally from the Taitung Canyon. Only minor amounts of sediments from the West Philippine Sea Basin, or from the Ryukyu Islands, are transported transversely to the southwestern Ryukyu Trench floor.

Transverse sediment dispersal

The elevation above the seafloor of the Yaeyama Ridge, at ~2,500 m below sea level (bsl), is higher than the seafloor in the parallel, E–W-trending series of forearc basins on the Yaeyama accretionary prism to its north: the Hoping (depocenter at ~3,000 m bsl), Nanao (~3,700 m bsl), East Nanao (~4,600 m bsl), and Hateruma (~3,500 m bsl) basins (Figs. 1 and 11). The Yaeyama Ridge is therefore a barrier to transport of sediments derived from the Ryukyu Islands downslope to the Ryukyu Trench; most of those sediments are mainly in the four forearc basins (Fig. 11). The post-Pleistocene sediments of the southwest Ryukyu Islands are mainly carbonate and siliciclastic rocks (Sagawa et al. 2001), and these have probably been transported transversely from north to south to fill the forearc basins (Fig. 11). The only known periods of metamorphism were during the Jurassic and Paleocene–Eocene in the Ryukyu Islands (Kizaki 1986), indicating that sediments derived from them would have little volcanic content.

Moreover, there are no prominent gullies or submarine canyons on the Yaeyama accretionary prism that cross or bypass the Yaeyama Ridge. The starved trench-slope basins north of the trench wedges (Figs. 8 and 9) provide indirect evidence that little or no sediment has bypassed the linear Yaeyama Ridge to be deposited in the trench wedge. No pyrrhotite derived from the Taiwan orogenic belt was found in surface sediment samples from the East Nanao Basin (Fig. 10a and b), indicating that sediments from the Taiwan orogenic belt are not presently being longitudinally transported to the East Nanao Basin. However, it is likely to find such pyrrhotite-bearing sediments in the Hoping and Nanao basins that are adjacent to Taiwan Island (Fig. 11).

Supporting evidence for two dispersal systems

In Taiwan, pyrrhotite is found in greenschist facies assemblages in rocks in the epizone in the central range, but not in coastal range rocks, which are primarily volcanic (Horng et al. 2012). Detrital pyrrhotite with a magnetic signature strongly indicative of origin from metamorphic rocks in the Taiwan orogenic belt was identified in a piston core from the trench wedge, but not in a core from the East Nanao Basin, which demonstrates the importance of the role of the large, river-connected submarine canyons (Hualien and Taitung) in the far-field delivery of terrestrial sediments from Taiwan to the southwestern Ryukyu Trench. Sediments derived from metamorphic facies containing pyrrhotite in the central range (shaded yellow in Fig. 11b) are transported by mainly fluvial processes to the Hualien and Peinan rivers (Dadson et al. 2005; Horng et al. 2012), which deliver those sediments to the heads of the Hualien and Taitung canyons, which in turn transport them for final deposition in the southwestern end of the Ryukyu Trench. The evidence of absence of pyrrhotite in the East Nanao Basin supports the notion that generally the sediment dispersal was separated into longitudinal and transverse systems in the southwestern Ryukyu arc–trench system by the Yaeyama Ridge at the present day. Usage of isotopes of minerals as a tracer of Taiwan terrigenous sources is also possible. The Pb–Sr and Zn isotope compositions of marine cores indicate the provenance of terrigenous detritus (Bentahila et al. 2008). The isotope results from core analysis and the presence of detrital pyrrhotite can be considered as supporting evidence to determine the percentage of the Taiwan orogenic source.

Conclusions

Bathymetric data, seismic profiles, and piston core sediment samples were used to identify two coexisting sediment dispersal systems in the southwestern Ryukyu arc–trench system. Deposition of sediments at the southwestern end of the trench is the end result of a longitudinal sediment dispersal system that carries sediments eroded from the Taiwan orogenic belt

eastward along the Hualien Canyon, with additional lateral supply of sediment from the Taitung Canyon. This demonstrates the important role of large submarine canyons in transporting terrestrial sediments from the Taiwan orogenic belt over long distances and delivering them to the western Ryukyu Trench. In contrast, deposition in the Hoping, Nanao, East Nanao, and Hateruma forearc basins is mainly a consequence of transverse downslope sediment transport from the Ryukyu Islands being blocked by the Yaeyama Ridge, which trends E–W along the trench-slope break. Pyrrhotite is a distinctive component of sediments derived from the Taiwan orogenic belt. Its presence in sediments from the trench, and its absence in sediments from the East Nanao Basin, support the view that the bulk of sediments deposited in the southwestern end of the Ryukyu Trench are derived from the Taiwan orogenic belt, and that those in the forearc basins are derived mostly from the Ryukyu Islands and the Yaeyama accretionary prism.

Acknowledgements The authors gratefully recognize the efforts of Captain Takafumi Aoki and the crew of R/V Kairei during the KR15-18 survey. The cruises YK15-01 and KR15-18 were supported by the research project for Compound Disaster Mitigation on the Great Earthquakes and Tsunamis Around the Nankai Trough Region of the Japanese Ministry of Education, Culture, Sports, Science and Technology, Japan. We thank the Ministry of Science and Technology, Taiwan, for permission to use bathymetric and seismic reflection data stored in the Ocean Data Bank, National Taiwan University, Taiwan. We are grateful to Prof. H.S. Yu for constructive comments on our interpretations of seismic reflection profiles. The article benefitted from helpful assessments by two reviewers.

Compliance with ethical standards

Conflict of interest The authors declare that there is no conflict of interest with third parties.

References

Abrahams SC, Calhoun BA (1953) The low-temperature transition in magnetite. Acta Crystallogr 6(1):105–106

Aiba J, Sekiya E (1979) Distribution and characteristics of the Neogene sedimentary basins around the Nansei-Shoto (Ryukyu Islands) (in Japanese with English abstract). J Japanese Assoc Petrol Technol 44:329–340

Angelier J (1986) Geodynamics of the Eurasia-Philippine Sea Plate Boundary: preface. Tectonophysics 125(1-3):IX–X

Bentahila Y, Othman DB, Luck JM (2008) Strontium, lead and zinc isotopes in marine cores as tracers of sedimentary provenance: a case study around Taiwan orogen. Chem Geol 248:62–82

Collot JY, Fisher MA (1991) The collision zone between the north d'Entrecasteaux ridge and the new Hebrides island arc 1. Sea beam morphology and shallow structure. J Geophys Res 96:4457–4478. doi:10.1029/90JB00715

Covault JA, Fildani A, Romans BW, McHargue T (2011) The natural range of submarine canyon-and-channel longitudinal profiles. Geosphere 7:313–332. doi:10.1130/GES00610.1

Dadson SJ, Hovius N, Chen H, Dade WB, Lin JC, Hsu ML, Lin CW, Horng MJ, Chen TC, Milliman J, Stark CP (2004) Earthquake-triggered increase in sediment delivery from an active mountain belt. Geology 32(8):733–736. doi:10.1130/G20639.1

Dadson S, Hovius N, Pegg S, Dade WB, Horng MJ, Chen H (2005) Hyperpycnal river flows from an active mountain belt. J Geophys Res Earth Surf 110(F4). doi:10.1029/2004JF000244

Damuth JE (1979) Migrating sediment waves created by turbidity currents in the northern South China Basin. Geology 7:520–523

Dekkers MJ, Mattéi JL, Fillion G, Rochette P (1989) Grain-size dependence of the magnetic behavior of pyrrhotite during its low-temperature transition at 34 K. Geophys Res Lett 16(8):855–858. doi:10.1029/GL016i008p00855

Deschamps AE, Lallemand SE, Collot JY (1998) A detailed study of the Gagua ridge: a fracture zone uplifted during a plate reorganisation in the mid-Eocene. Mar Geophys Res 20(5):403–423. doi:10.1023/A:1004650323183

Dominguez S, Lallemand S, Malavieille J, Schnürle P (1998) Oblique subduction of the Gagua ridge beneath the Ryukyu accretionary wedge system: insights from marine observations and sandbox experiments. Mar Geophys Res 20(5):383–402. doi:10.1023/A:1004614506345

Eakin DH, McIntosh KD, Van Avendonk HJA, Lavier L (2015) New geophysical constraints on a failed subduction initiation: the structure and potential evolution of the Gagua ridge and Huatung Basin. Geochem Geophys Geosyst 16(2):380–400. doi:10.1002/2014GC005548

Font Y, Liu CS, Schnurle P, Lallemand S (2001) Constraints on backstop geometry of the southwest Ryukyu subduction based on reflection seismic data. Tectonophysics 333(1):135–158. doi:10.1016/S0040-1951(00)00272-9

Gohl K, Nitsche F, Miller H (1997) Seismic and gravity data reveal tertiary interplate subduction in the Bellingshausen Sea, southeast Pacific. Geology 25(4):371–374

Hayes DE, Lewis SD (1984) A geophysical study of the Manila trench, Luzon, Philippines 1. Crustal structure, gravity, and regional tectonic evolution. J Geophys Res 89(B11):9171–9195. doi:10.1029/JB089iB11p09171

Hinderer M (2012) From gullies to mountain belts: a review of sediment budgets at various scales. Sediment Geol 280:21–59. doi:10.1016/j.sedgeo.2012.03.009

Ho CS (1986) A synthesis of the geologic evolution of Taiwan. Tectonophysics 125:1–16. doi:10.1016/0040-1951(86)90004-1

Horng CS, Roberts AP (2006) Authigenic or detrital origin of pyrrhotite in sediments?: resolving a paleomagnetic conundrum. Earth Planet Sci Lett 241:750–762. doi:10.1016/j.epsl.2005.11.008

Horng CS, Huh CA, Chen KH, Lin CH, Shea KS, Hsiung KH (2012) Pyrrhotite as a tracer for denudation of the Taiwan orogen. Geochem Geophys Geosyst 13(8):Q08Z47. doi:10.1029/2012GC004195

Hsiung K-H, Yu H-S (2011) Morpho-sedimentary evidence for a canyon–channel–trench interconnection along the Taiwan–Luzon plate margin, South China Sea. Geo-Mar Lett 31:215–226. doi:10.1007/s00367-010-0226-7

Hsiung KH, Yu HS (2013) Sediment dispersal system in the Taiwan–South China Sea collision zone along a convergent margin: a comparison with the Papua New Guinea collision zone of the western Solomon Sea. J Asian Earth Sci 62:295–307. doi:10.1016/j.jseaes.2012.10.006

Hsiung KH, Yu HS, Su M (2015) Sedimentation in remnant ocean basin off southwest Taiwan with implication for closing northeastern South China Sea. J Geol Soc 172:641–647. doi:10.1144/jgs2014-077

Jabaloy A, Balanyá JC, Barnolas A, Galindo-Zaldıvar J, Hernández-Molina FJ, Maldonado A, Martínez-Martíneza JM, Rodríguez-Fernández J, de Galdeano CS, Somoza L, Suriñach E, Vázquez JT (2003) The transition from an active to a passive margin (SW end of the south Shetland trench, Antarctic Peninsula). Tectonophysics 366(1):55–81. doi:10.1016/S0040-1951(03)00060-X

Jarrard RD (1986) Relations among subduction parameters. Rev Geophys 24:217–284. doi:10.1029/RG024i002p00217

Karig DE (1973) Plate convergence between the Philippines and the Ryukyu Islands. Mar Geol 14(3):153–168. doi:10.1016/0025-3227(73)90025-X

Karig DE, Sharman GF (1975) Subduction and accretion in trenches. Geol Soc Am Bull 86(3):377–389

Kizaki K (1986) Geology and tectonics of the Ryukyu Islands. Tectonophysics 125(1):193–207. doi:10.1016/0040-1951(86)90014-4

Lallemand S, Liu CS, Dominguez S, Schnürle P, Malavieille J (1999) Trench-parallel stretching and folding of forearc basins and lateral migration of the accretionary wedge in the southern Ryukyus: a case of strain partition caused by oblique convergence. Tectonics 18(2): 231–247. doi:10.1029/1998TC900011

Lash GG (1985) Recognition of trench fill in orogenic flysch sequences. Geology 13(12):867–870

Lehu R, Lallemand S, Hsu SK, Babonneau N, Ratzov G, Lin AT, Dezileau L (2015) Deep-sea sedimentation offshore eastern Taiwan: facies and processes characterization. Mar Geol 369:1–18. doi:10.1016/j.margeo.2015.05.013

Lewis KB (1994) The 1500-km-long Hikurangi Channel: trench-axis channel that escapes its trench, crosses a plateau, and feeds a fan drift. Geo-Mar Lett 14(1):19–28. doi:10.1007/BF01204467

Lewis SD, Hayes DE (1989) Plate convergence and deformation, north Luzon ridge, Philippines. Tectonophysics 168(1-3):221–237. doi: 10.1016/0040-1951(89)90377-6

Macdonald DIM (1993) Controls on sedimentation at convergent plate-margins. In: Frostick LE, Stell RJ (eds) Tectonic controls and signatures in sedimentary successions. Blackwell, Oxford, pp 225–257

Malatesta C, Gerya T, Crispini L, Federico L, Capponi G (2013) Oblique subduction modelling indicates along-trench tectonic transport of sediments. Nat Commun 4:2456. doi:10.1038/ncomms3456

Malavieille J, Lallemand SE, Dominguez S, Deschamps A, Lu CY, Liu CS, Schnürle P (2002) Arc-continent collision in Taiwan: new marine observations and tectonic evolution. In: Byrne TB, Liu CS (eds) Geology and geophysics of an arc-continent collision, Taiwan, republic of China. Geol Soc Am Spec Pap 358:189–213

Maldonado A, Larter RD, Aldaya F (1994) Forearc tectonic evolution of the south Shetland margin, Antarctic Peninsula. Tectonics 13(6): 1345–1370. doi:10.1029/94TC01352

MARGINS (2004) MARGINS Science Plans 2004. http://www.nsf-margins.org/S2S/S2S.html

McIntosh KD, Nakamura Y (1998) Crustal structure beneath the Nanao forearc basin from TAICRUST MCS/OBS line 14. Terr Atmos Ocean Sci 9(3):345–362

Milliman JD, Lin SW, Kao SJ, Liu JP, Liu CS, Chiu JK, Lin YC (2007) Short-term changes in seafloor character due to flood-derived hyperpycnal discharge: typhoon Mindulle, Taiwan, July 2004. Geology 35(9):779–782. doi:10.1130/G23760A.1

Milsom J, Masson D, Nicols G (1992) Three trench endings in eastern Indonesia. Mar Geol 104(1):227–241. doi:10.1016/0012-821X(87)90009-4

Mountney NP, Westbrook GK (1996) Modelling sedimentation in ocean trenches: the Nankai trough from 1 ma to the present. Basin Res 8(1):85–101. doi:10.1111/j.1365-2117.1996.tb00116.x

Nichols G, Hall R, Milsom J, Masson D, Parson L, Sikumbang N, Dwiyanto B, Kallagher H (1990) The southern termination of the Philippine trench. Tectonophysics 183(1-4):289–303. doi:10.1016/0040-1951(90)90422-5

Okada H (1989) Anatomy of trench-slope basins: examples from the Nankai trough. Palaeogeogr Palaeoclimatol Palaeoecol 71(1-2):3–13. doi:10.1016/0031-0182(89)90026-6

Pickering KT, Hiscott RN (2015) Deep marine systems: processes, deposits, environments, tectonics and sedimentation. Wiley, Chichester

Rochette P (1987) Metamorphic control of the magnetic mineralogy of black shales in the Swiss alps: toward the use of "magnetic isograde". Earth Planet Sci Lett 84(4):446–456. doi:10.1016/0012-821X(87)90009-4

Sagawa N, Nakamori T, Iryu Y (2001) Pleistocene reef development in the southwest Ryukyu Islands, Japan. Palaeogeogr Palaeoclimatol Palaeoecol 175(1):303–323. doi:10.1016/S0031-0182(01)00377-7

Schnürle P, Liu CS, Lallemand SE, Reed DL (1998a) Structural insight into the south Ryukyu margin: effects of the subducting Gagua ridge. Tectonophysics 288(1):237–250. doi:10.1016/S0040-1951(97)00298-9

Schnürle P, Liu CS, Lallemand SE, Reed DL (1998b) Structural controls of the Taitung canyon in the Huatung Basin east of Taiwan. Terr Atmos Ocean Sci 9(3):453–472

Smoczyk GM, Hayes GP, Hamburger MW, Benz HM, Villaseñor A, Furlong KP (2013) Seismicity of the Earth 1900-2012 Philippine Sea plate and vicinity. US Geological Survey, No. 2010-1083-M

Soh W, Machiyama H, Shirasaki Y, Kasahara J (2004) Deep-sea floor instability as cause of deep-water cable fault, off eastern part of Taiwan. Frontier Res Earth Evol 2:1–8

Sømme TO, Helland-Hansen W, Martinsen OJ, Thurmond JB (2009) Relationships between morphological and sedimentological parameters in source-to-sink systems: a basis for predicting semi-quantitative characteristics in subsurface systems. Basin Res 21(4): 361–387. doi:10.1111/j.1365-2117.2009.00397.x

Spinelli GA, Mozley PS, Tobin HJ, Underwood MB, Hoffman NW, Bellew GM (2007) Diagenesis, sediment strength, and pore collapse in sediment approaching the Nankai trough subduction zone. Geol Soc Am Bull 119(3-4):377–390. doi:10.1130/B25920.1

Stern RJ (2002) Subduction zones. Rev Geophys 40:1012. doi:10.1029/2001RG000108

Su M, Hsiung KH, Zhang C, Xie X, Yu HS, Wang Z (2015) The linkage between longitudinal sediment routing systems and basin types in the northern South China Sea in perspective of source-to-sink. J Asian Earth Sci 111:1–13. doi:10.1016/j.jseaes.2015.05.011

Suppe J (1981) Mechanics of mountain building and metamorphism in Taiwan. Mem Geol Soc China 4:67–89

Thornburg TM, Kulm LD (1987) Sedimentation in the Chile trench: depositional morphologies, lithofacies, and stratigraphy. Geol Soc Am Bull 98(1):33–52

Thornburg TM, Kulm LD, Hussong DM (1990) Submarine-fan development in the southern Chile trench: a dynamic interplay of tectonics and sedimentation. Geol Soc Am Bull 102(12):1658–1680

Ujiie H, Tanaka Y, Ono T (1991) Late quaternary paleoceanographic record from the middle Ryukyu trench slope, northwest Pacific. Mar Micropaleontol 18(1):115–128. doi:10.1016/0377-8398(91)90008-T

Ujiie H, Nakamura T, Miyamoto Y, Park JO, Hyun S, Oyakawa T (1997) Holocene turbidite core from the southern Ryukyu trench slope: suggestions of periodic earthquakes. J Geol Soc Japan 103(6):590–603

Underwood MB, Karig DE (1980) Role of submarine canyons in trench and trench-slope sedimentation. Geology 8(9):432–436

Underwood MB, Ballance PF, Clift PD, Hiscott RN, Marsaglia KM, Pickering KT, Reid RP (1995) Sedimentation in forearc basins, trenches, and collision zones of the western Pacific: a summary of results from the ocean drilling program. In: Active Margins and Marginal Basins of the Western Pacific, pp 315–353

Van Avendonk HJA, Kuo-Chen H, McIntosh KD, Lavier LL, Okaya DA, Wu FT, Wang CY, Lee CS, Liu CS (2014) Deep crustal structure of an arc-continent collision: constraints from seismic traveltimes in central Taiwan and the Philippine Sea. J Geophys Res Solid Earth 119(11):8397–8416. doi:10.1002/2014JB011327

Von Huene R (1986) To accrete or not accrete, that is the question. Geol Rundsch 75(1):1–15

Wessel P, Smith WHF, Scharroo R, Luis J, Wobbe F (2013) Generic mapping tools: improved version released. EOS Trans Am Geophys Union 94(45):409–410

Whitmore GP, Crook KAW, Johnson DP (1999) Sedimentation in a complex convergent margin: the Papua New Guinea collision zone of the western Solomon Sea. Mar Geol 157:19–45. doi:10.1016/S0025-3227(98)00132-7

Wu S, Takahashi N, Tokuyama H, Wong HK (2005) Geomorphology, sedimentary processes and development of the Zenisu deep-sea channel, northern Philippine Sea. Geo-Mar Lett 25(4):230–240. doi:10.1007/s00367-005-0210-9

Yu HS (2003) Geological characteristics and distribution of submarine physiographic features in the Taiwan region. Mar Georesour Geotechnol 21(3-4):139–153. doi:10.1080/713773391

Yu HS, Chiang CS, Shen SM (2009) Tectonically active sediment dispersal system in SW Taiwan margin with emphasis on the Gaoping (Kaoping) submarine canyon. J Mar Syst 76:369–382. doi:10.1016/j.jmarsys.2007.07.010